2-12-2015

Analysis of the Surface Density and Reactivity of Perfluorophenylazide and the Impact on Ligand Immobilization

Gilad Zorn
University of Washington

David G. Castner
University of Washington

Anuradha Tyagi
Portland State University

Xin Wang
Portland State University

Hui Wang
Portland State University

See next page for additional authors

Citation Details

Zorn, G., Castner, D. G., Tyagi, A., Wang, X., Wang, H., & Yan, M. (2015). Analysis of the surface density and reactivity of perfluorophenylazide and the impact on ligand immobilization. Journal of Vacuum Science & Technology A,33(2), 021407. and may be found at http://dx.doi.org/10.1116/1.4907924

Analysis of the surface density and reactivity of perfluorophenylazide and the impact on ligand immobilization

Gilad Zorn[a] and David G. Castner
National ESCA and Surface Analysis Center for Biomedical Problems, Departments of Bioengineering and Chemical Engineering, University of Washington, Box 351653, Seattle, Washington 98195-1653

Anuradha Tyagi, Xin Wang, Hui Wang, and Mingdi Yan[b]
Department of Chemistry, Portland State University, Portland, Oregon 97207-0751

(Received 18 December 2014; accepted 30 January 2015; published 12 February 2015)

Perfluorophenylazide (PFPA) chemistry is a novel method for tailoring the surface properties of solid surfaces and nanoparticles. It is general and versatile, and has proven to be an efficient way to immobilize graphene, proteins, carbohydrates, and synthetic polymers. The main thrust of this work is to provide a detailed investigation on the chemical composition and surface density of the PFPA tailored surface. Specifically, gold surfaces were treated with PFPA-derivatized (11-mercaptoundecyl)tetra(ethylene glycol) (PFPA-MUTEG) mixed with 2-[2-(2-mercaptoethoxy)ethoxy]ethanol (MDEG) at varying solution mole ratios. Complementary analytical techniques were employed to characterize the resulting films including Fourier transform infrared spectroscopy to detect fingerprints of the PFPA group, x-ray photoelectron spectroscopy and ellipsometry to study the homogeneity and uniformity of the films, and near edge x-ray absorption fine structures to study the electronic and chemical structure of the PFPA groups. Results from these studies show that the films prepared from 90:10 and 80:20 PFPA-MUTEG/MDEG mixed solutions exhibited the highest surface density of PFPA and the most homogeneous coverage on the surface. A functional assay using surface plasmon resonance with carbohydrates covalently immobilized onto the PFPA-modified surfaces showed the highest binding affinity for lectin on the PFPA-MUTEG/MDEG film prepared from a 90:10 solution. © *2015 American Vacuum Society*.
[http://dx.doi.org/10.1116/1.4907924]

I. INTRODUCTION

Perfluorophenylazide (PFPA) has been recently used to immobilize functional groups onto solid surfaces and nanoparticles. The versatility of the PFPA chemistry makes it an attractive choice for surface modification upon thermal activation or light irradiation of the azide functionality.[1–12] The PFPA immobilization method is simple, reproducible, and has been proven to be efficient to immobilize synthetic polymers,[1] graphene,[2,3] and carbohydrates[4–7] onto variety of surfaces.[8] Moreover, PFPA allows controlling the surface density of the immobilized molecules through adjustment of the PFPA solution concentration.[9,10] The efficiency of the surface coupling is directly related to the surface density of the PFPA groups. Optimal surface density increases the coupling efficiency and should result in enhanced interactions with their binding partners. Thiol-gold bonding is a convenient, well-defined model system for modifying surfaces and immobilizing functional molecules onto surfaces,[13,14] and therefore, thiol-functionalized PFPAs were chosen to optimize the binding affinity of PFPA. In particular, PFPA derivatized with (11-mercaptoundecyl)tetra(ethylene glycol) (PFPA-MUTEG) was synthesized for ligand immobilization (Fig. 1).[7] The surface density of the PFPA groups as well as the impact of PFPA density on the surface reactivity were studied by adding different mole ratios of 2-[2-(2-mercaptoethoxy)ethoxy]ethanol (MDEG) (Fig. 1) to the PFPA-MUTEG solutions. In general, the adsorption from mixed thiol solutions allows the formation of monolayers with widely varying compositions.[13,15–17] The surface density of a specific adsorbate does not necessarily follow its mole fraction in solution through all concentration ranges. The choice of solvents or thiol chain length, for example, can bias the surface density of one adsorbate.[13,18–20] Hence, it is important to analyze the structure and composition of the generated surfaces. The monolayers were adsorbed onto gold surfaces from PFPA-MUTEG/MDEG mixed solutions. These films were studied in detail with Fourier transform infrared spectroscopy (FTIR), x-ray photoelectron spectroscopy (XPS), ellipsometry, and near edge x-ray absorption fine structure (NEXAFS). Carbohydrates were then covalently immobilized onto the modified surfaces, and their interactions with lectin were studied by surface plasmon resonance imaging (SPRi). The correlation between PFPA surface density and carbohydrate immobilization efficiency was subsequently established.

II. EXPERIMENT

A. Materials

Standard chemicals were purchased from commercial suppliers and used as received. The long-pass optical filter (280 nm) and high refractive index N-SF10 glass slides

[a]Present address: General Electric Global Research, One Research Circle, Niskayuna, NY 12309; electronic mail: zorn@ge.com
[b]Present address: Department of Chemistry, University of Massachusetts Lowell, One University Ave., Lowell, MA 01854; electronic mail: Mingdi_Yan@uml.edu

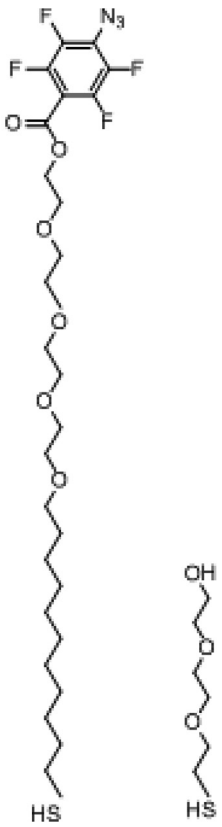

PFPA-MUTEG MDEG

FIG. 1. Molecular structures of PFPA-MUTEG and MDEG.

(18 mm × 18 mm × 1 mm) were purchased from Schott Glass Technologies, Inc. (Fullerton, CA). PFPA-MUTEG and MDEG (Fig. 1) were synthesized following the procedures that were described elsewhere.[5]

3,6-di-O-(α-D-Mannopyranosyl)–D-mannopyranose (Man3, V-Labs Inc., Covington, LA), 2-O-α-D-mannopyranosyl-D-mannopyranose (Man2, Sigma), D-mannose (Man, Fluka), D-glucose (Glc, TCI), and D-galactose (Gal, TCI) were used as received. Concanavalin A (Con A) from jack-bean *Canavalia ensiformis* (104 kDa, Sigma) was used without further purification. A stock solution of Con A (3.85 μM) was prepared in *p*H 7.4 PBS buffer (1.7 mM NaH_2PO_4, 8.2 mM Na_2HPO_4, and 150 mM NaCl).

B. Sample preparation

Gold substrates were fabricated by coating Au films on high refractive index N-SF10 glass. The slides were cleaned in piranha solution (3:1, v/v, conc. H_2SO_4/H_2O_2) at r.t. for 60 min. (Caution: the piranha solution reacts vigorously with organic solvents.) The slides were thoroughly washed in boiling water three times for 60 min each. The slides were then coated with a 2 nm thick Ti adhesion layer followed by a 45 nm thick gold film in an electron beam evaporator (SEC-600, CHA) at the Washington Nanofabrication Facility (University of Washington). Immediately before they were chemically functionalized, these substrates were cleaned by soaking them in the piranha solution for 30–45 s at 35 °C followed by washing in boiling water three times for 20 min each. The substrates were then washed with milli-Q water followed by ethanol before soaking in the thiol solution for monolayer formation. Stock solutions of PFPA-MUTEG (10 mM) and MDEG (28 mM) were prepared by dissolving the corresponding compound in ethanol. For film preparation, the total concentration of the thiol solution was kept at 4 mM for either 100% PFPA-MUTEG or the mixtures of PFPA-MUTEG and MDEG. Substrates were then soaked in the thiol solution at room temperature for 3 h followed by gentle washing in ethanol three times for 5 min each, and dried with nitrogen. Carbohydrates were fabricated on SPR sensors as described elsewhere.[5] Briefly, stock solutions of carbohydrates prepared in milli-Q water were printed onto PFPA-functionalized SPR chips with a 360 μm capillary pin under a constant 60% humidity using a robotic printer (BioOdyssey Calligrapher miniarrayer, Bio-Rad Laboratories, Inc.). The chip was then irradiated with a 450 W medium pressure Hg lamp (Hanovia) for 5 min in the presence of a 280 nm optical filter, rinsed gently with water for three times, and dried with N_2.

C. FTIR

FTIR measurements were performed using a Bruker Tensor spectrometer with a germanium attenuated total reflectance crystal in the mid-IR frequency range (4000–400 cm^{-1}). Each spectrum was acquired using 1000 scans at 4 cm^{-1} resolution, and the data were analyzed using OPUS software.

D. XPS

XPS measurements were performed on a Kratos AXIS Ultra DLD instrument (Kratos, Manchester, England) employing a hemispherical analyzer and using a monochromatic Al Kα x-ray source in the hybrid mode (large acceptance angle of photoelectrons). Compositional survey scans were acquired using pass energy of 80 eV and a nominal 0° takeoff angle (TOA). The TOA is defined as the angle between the sample surface normal and the axis of the XPS analyzer lens. A coaxial filament was used to produce low energy electrons for charge neutralization during all measurements. Three spots on two or more replicates of each sample type were analyzed. The compositional data are an average of the values determined at each spot. Compositions were calculated with the CasaXPS software.

E. Ellipsometry

Thickness measurements were made on a model LSE Stokes ellipsometer (Gaertner Scientific Corporation, Skokie, IL, USA) with wavelength of 6.328 Å (He/Ne laser) and incidence angle of 70°. The thickness was obtained by taking the average of the readings from three different spots on the sample surface.

F. NEXAFS

NEXAFS spectra were collected at the U7A beamline at the National Synchrotron Light Source (NSLS, Brookhaven National Laboratory, Upton, NY) using an elliptically ~85%

p-polarized beam. The beam line is equipped with a monochromator and a 600 l/mm grating that provides a full-width at half maximum resolution of ~0.15 eV at the carbon K-edge (285 eV). The monochromator energy scale was calibrated using the 285.35 eV C1s to π^* transition on a graphite transmission grid and partial electron yields were divided by the beam flux during data acquisition.[21] A detector with a bias voltage set at −250 V for the C K-edge was used to monitor the partial electron yield. All spectra were normalized to an edge step height of unity.

G. SPRi

SPRi experiments were performed on a SPR imager®II (GWC Technologies, Madison, WI) at room temperature and at a flow rate of 100 μl/min. The experiments were carried out following the procedure as described elsewere.[5] Briefly, the substrates with the carbohydrate ligands were flushed with *p*H 7.4 PBS buffer followed by a solution of BSA in *p*H 7.4 PBS buffer (2 μM), after which, the PBS buffer was introduced again until a flat baseline was obtained. A solution of Con A in *p*H 7.4 PBS was introduced to the flow cell for about 3 min. The running solution was then switched to the PBS buffer followed by 8 M urea solution to regenerate the array surface. The sequence, PBS/BSA/PBS/ConA/PBS/urea/PBS, was then repeated to test the regenerated surface for reproducibility.

III. RESULTS AND DISCUSSION

Five solutions were prepared to vary the surface density of PFPA: 100% PFPA-MUTEG, three mixtures of PFPA-MUTEG and MDEG at solution mole ratios of 90:10, 80:20, and 50:50, and 100% MDEG. Organic films were then assembled from these solutions onto gold surfaces and FTIR was applied to detect the successful attachment of these films. Figure 2(a) shows the FTIR spectra of the 100% PFPA-MUTEG film, 100% MDEG film, and the three mixed films prepared from 90:10, 80:20, and 50:50 solutions. The characteristic azide peak near 2125 cm^{-1} (Refs. 12 and 16) (labeled 1) is absent, as expected, in the spectrum of the 100% MDEG film. This peak is very weak for the PFPA-MUTEG/MDEG mixed film prepared from a 50:50 solutions due to low azide surface concentration in this PFPA-MUTEG film. On the other hand, the azide absorption was observed in the 100% PFPA-MUTEG film as well as the PFPA-MUTEG/MDEG mixed

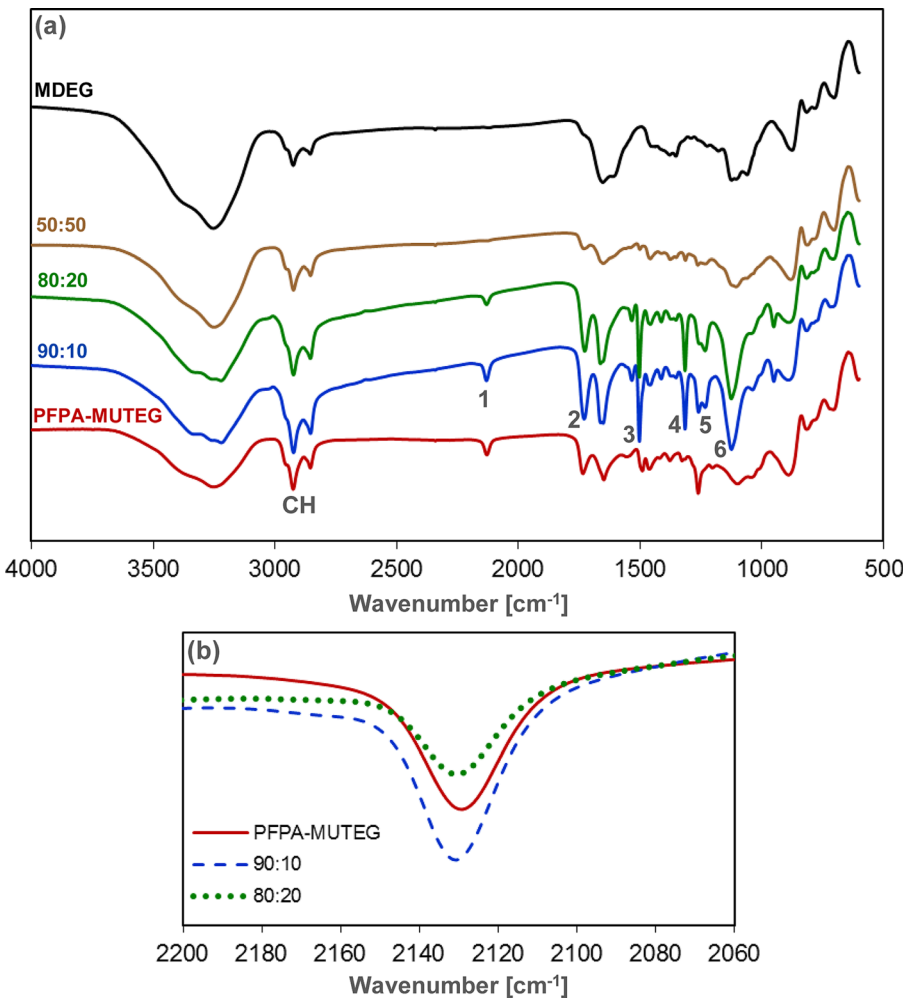

FIG. 2. (Color online) (a) FTIR spectra of 100% PFPA-MUTEG film, 100% MDEG film, as well as PFPA-MUTEG/MDEG mixed films prepared from 90:10, 80:20, and 50:50 solutions. (b) FTIR azide peak of 100% PFPA-MUTEG film and PFPA-MUTEG/MDEG mixed films prepared from 90:10 and 80:20 solutions.

TABLE I. XPS determined elemental compositions without the gold signal from the substrate compared to the expected stoichiometric elemental compositions.

	Stoichiometric atomic percent (calculated)		Atomic percent measured by XPS				
	PFPA	MDEG	100% PFPA-MUTEG	PFPA:MDEG 90:10	PFPA:MDEG 80:20	PFPA:MDEG 50:50	100% MDEG
N	7.5	—	7.3	3.9	4.3	4.3	—
F	10.0	—	8.6	10.6	10.8	2.6	—
S	2.5	10.0	2.0	1.2	1.4	0.7	4.6
C	65.0	60.0	64.0	66.9	64.7	73.4	65.6
O	15.0	30.0	18.1	17.5	17.9	19.1	29.8

films prepared from 90:10 and 80:20 solutions. From comparing the intensity of the azide peak of the 100% PFPA-MUTEG film with the mixed films [Fig. 2(b)], it is clearly seen that the strongest intensity was observed for the PFPA-MUTEG/MDEG mixed film prepared from 90:10 solution. This indicates that this mixed film contained the highest surface concentration of PFPA. A similar trend was observed for the carbonyl peak around 1740 cm^{-1} (Refs. 22 and 23) (labeled 2) and for the aromatic symmetric stretches at around 1500 cm^{-1} (labeled 3) as well as the ring asymmetric stretches at ~1320 cm^{-1} (labeled 4).[22] Moreover, the peaks that are assigned to the aromatic Ar-F stretching at ~1220 cm^{-1} (labeled 5) and at ~1110 cm^{-1} (labeled 6)[22] all showed higher intensities for the PFPA-MUTEG/MDEG mixed films prepared from 90:10 and 80:20 solutions as compared to the 100% PFPA-MUTEG film. In addition, the methylene stretching frequencies are characteristics for the degree of ordering in organic layers.[24–27] Measured methylene asymmetric stretching frequencies of 2920 cm^{-1} for the PFPA-MUTEG/MDEG mixed films prepared from 90:10 and 80:20 solutions versus a value of 2924 cm^{-1} for the 100% PFPA-MUTEG suggest that the mixed film have a slightly higher degree of order.

XPS was used to gain further understanding regarding the chemical composition of these films. Elemental compositions (Table S1, supplementary material)[28] show as expected that the 100% PFPA-MUTEG and the three mixed films (prepared 90:10, 80:20, and 50:50 solutions) contained N, F, C, O, and S from the films,[2,12] as well as Au from the substrate. It is should be noted that quantitative information based on the N signal is limited as the azide decomposes under the x-ray measurement[29] and this may be the reason for the decrease in the nitrogen atomic percentages in the mixed films prepared from 90:10 and 80:20 solutions compared to the 100% film (Table S1, supplementary material).[28] Table I shows the XPS determined elemental compositions without the gold signal from the substrate compared to the expected stoichiometric elemental compositions of PFPA-MUTEG and MDEG. This table provides insight about where various elements are located in the film. The measured S concentration is significantly lower than the stoichiometric value, indicating S is located near the Au substrate. The C, O, and F XPS compositions are very close to the expected stoichiometric compositions indicating that the PFPA films have a fairly homogeneous composition. The C/Au ratio is a good indication of the film thickness/density and homogeneity. A higher value corresponds to higher presentation of the organic molecules covering the gold substrate and smaller standard deviation values indicate improved homogeneity of the organic layer across the gold substrate. While comparing the C/Au ratios for the different films (Table II), it is clear that the 100% PFPA-MUTEG film was thinner or less dense than the PFPA-MUTEG/MDEG mixed films prepared from 90:10 and 80:20 solutions. This is consistent with the significant decrease in the measured Au composition of the mixed films prepared from 90:10 and 80:20 solutions, compared to the 100% PFPA-MUTEG (Table S1, supplementary material).[28] The F/Au ratio followed the same trend providing additional confirmation that the PFPA-MUTEG/MDEG mixed films prepared from 90:10 and 80:20 solutions contained higher surface concentrations of PFPA-MUTEG. Moreover, the 100% PFPA-MUTEG film had higher standard deviation values, indicating a less homogenous coverage of the organic layer.

To determine the thickness of the different films, ellipsometry measurements were performed.[20,26,27,30,31] The measured values were 26.2 ± 1 Å for 100% PFPA-MUTEG, 29.0 ± 0.3 Å and 28.9 ± 1 Å for the PFPA-MUTEG/MDEG mixed films prepared from 90:10 and 80:20 solutions, respectively. Consistent with the XPS results, the 90:10 and 80:20 PFPA-MUTEG/MDEG solutions produced the thickest films.

NEXAFS carbon K-edge spectra for the 100% PFPA-MUTEG films as well as the mixed PFPA-MUTEG/MDEG films prepared from 90:10 and 80:20 solutions acquired at an angle of 55° between the incident x-ray beam and the surface plan are shown in Fig. 3. This is the NEXAFS "magic angle" and is typically used to compare differences in bonding features among samples.[21] All three spectra exhibit a characteristic resonance near 285 eV, and for the two mixed films this peak is split into peaks at 284.9 and 285.9 eV (labeled 1 and 2). This resonance is commonly related to the π^* resonance

TABLE II. XPS C/Au, F/Au and F/C atomic ratios of 100% PFPA-MUTEG film, 100% MDEG film, and PFPA-MUTEG/MDEG mixed films prepared from solution concentrations of 90:10, 80:20, and 50:50.

	XPS atomic ratios				
	100% PFPA-MUTEG	90:10	80:20	50:50	100% MDEG
C/Au	1.3 ± 0.5	2.2 ± 0.2	2.1 ± 0.2	0.72 ± 0.1	0.7 ± 0.2
F/Au	0.16 ± 0.04	0.35 ± 0.04	0.35 ± 0.05	0.04 ± 0.01	—
F/C	0.14 ± 0.05	0.16 ± 0.001	0.17 ± 0.01	0.05 ± 0.02	—

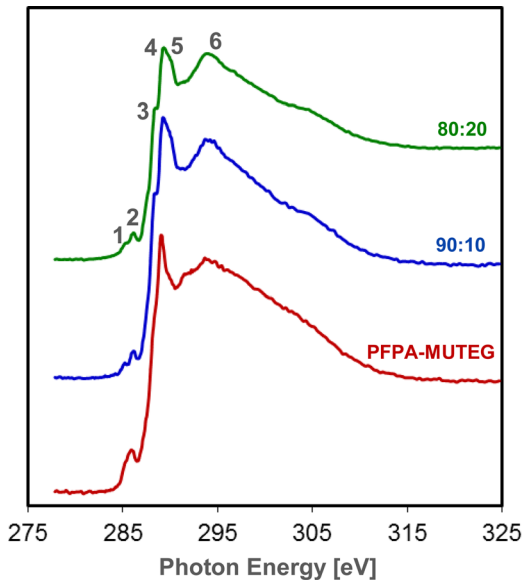

FIG. 3. (Color online) NEXAFS carbon K-edge spectra acquired at x-ray incident angle of 55° for the 100% PFPA-MUTEG film, as well as the PFPA-MUTEG/MDEG mixed films prepared from 90:10 and 80:20 solutions.

from C=C bonds.[32–38] However, upon fluorination, the π^* C=C resonance is shifted by as much as 5 eV,[21,37] and therefore, the peak at 289.2 eV (labeled 4) is also related with the F-C*=C-F π^* resonance. In addition, the two PFPA-MUTEG/MDEG mixed films present a shoulder at 288.2 eV (labeled 3) and a peak at 289.8 (labeled 5). Previous NEXAFS studies of aromatic molecules showed a split of π^* resonance to π^*_1 and π^*_2 that may be resulted from resonance interaction between localized molecular states.[21,33,38] Thus, it is likely that the peaks at 288.2, 289.2, and 289.8 eV (labeled 3–5) are related to F-C=C-F and F-C=C-N π^* resonances, and the peak at 285.9 eV (labeled 2) is related to C=O π^* resonance. The peak at 293.8 eV (labeled 6) corresponds to the C-C σ^* transition.[38] By comparing the spectra for the 100% PFPA-MUTEG film to the mixed PFPA-MUTEG/MDEG films prepared from 90:10 and 80:20 solutions, it is clearly seen that the peaks that are related to the PFPA aromatic structure (labeled 1, 3, and 5) are much stronger in the spectra of the mixed films. Their appearance in the mixed films spectra can be attributed to the increased surface density of the PFPA-MUTEG upon assembly in the presence of the shorter MDEG spacer.

FTIR, XPS, ellipsometry, and NEXAFS all show that PFPA-MUTEG/MDEG mixed films prepared from 90:10 and 80:20 solutions present higher surface density of PFPA groups as compared to the films prepared from 100% PFPA-MUTEG solution. In addition, FTIR methylene stretching frequencies suggest that orientation effects also result in the higher surface density of the PFPA on the PFPA-MUTEG/MDEG mixed films prepared from 90:10 and 80:20 solutions. A possible explanation to the higher PFPA surface density after slightly diluting the PFPA-MUTEG solution with the MDEG is the fact that the PFPA-MUTEG chains are relatively long and flexible and the addition of short MDEG chains serves as a spacer facilitating the chain packing, thus increasing the packing density and order of the resulting film. Following this assumption, additional study was performed by diluting the PFPA-MUTEG solutions with MUTEG, which has similar molecular length as compared to PFPA-MUTEG and is much longer than the MDEG spacer. The molecular structure of MUTEG is provided in Fig. S1 (supplementary material)[28] and Table S2 (supplementary material)[28] provides the XPS determined surface elemental compositions of the film prepared from 100% MUTEG solution as well as a mixed film prepared from 90:10 solution of PFPA-MUTEG and MUTEG. As shown Table S2 (supplementary material),[28] the surface compositions of the films prepared from 100% MUTEG and 90:10 PFPA-MUTEG/MUTEG solutions are similar, indicating that the film prepared from 90:10 PFPA-MUTEG/MUTEG solution contains mainly MUTEG molecules. PFPA-MUTEG and MUTEG have similar length but the smaller head group of the later leads to preferred adsorption of the MUTEG molecules on the gold surface even when only 10% are presented in the solution. Unlike the longer MUTEG, MDEG is much shorter and therefore acts as a spacer and allows coadsorption with PFPA-MUTEG and as a result improves packing density, orientation and order of the PFPA groups on the films that were prepared from 90:10 and 80:20 PFPA-MUTEG/ MDEG solutions.

The detailed surface study did not reveal significant differences between the PFPA-MUTEG/MDEG mixed films prepared from 90:10 and 80:20 solutions and therefore additional analysis was required to distinguish between the immobilization efficiencies of these two mixed films. To investigate whether the PFPA density would impact the subsequent immobilization, and whether there are differences in surface affinity between the PFPA-MUTEG/MDEG mixed films prepared from 90:10 and 80:20 solutions, carbohydrates were coupled onto the PFPA-modified Au surfaces. Man3, Man2, Man, Glc, and Gal were printed on PFPA-functionalized SPR sensors in quadruplets in a 5×4 array and were then immobilized by photoactivation.[8] Functional assays were carried out by exposing the carbohydrate microarray to the Con A solution and SPR responses were recorded (Fig. 4). Con A is a lectin that exhibits

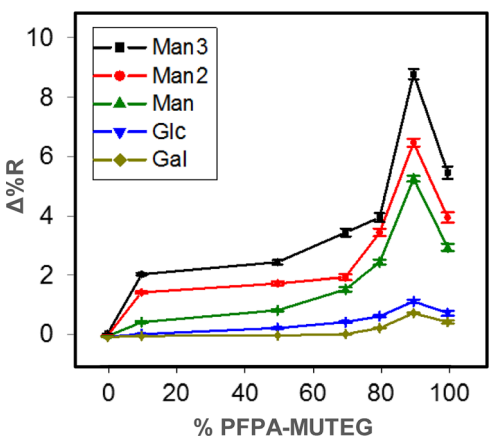

FIG. 4. (Color online) SPRi responses, in percent change in reflectivity (Δ%R), of a carbohydrate microarray to Con A. Carbohydrates were immobilized on SPRi sensor chips treated with PFPA-MUTEG/MDEG. Each data point was an average of the four duplicate spots on the microarray. The lines were drawn to aid visualization.

high affinity for carbohydrates having a terminal α-D-Mannopyranosyl group.[39] Glc is also a binder to Con A, although the affinity is weaker than Man, and Gal is a nonbinder to Con A. It is clearly observed in Fig. 4 that the strongest signals (i.e., highest binding affinity) were measured for carbohydrates immobilized on the PFPA-MUTEG/MDEG films prepared from 90:10 solutions. The surface densities and uniformities of PFPA in the mixed films prepared from the 90:10 and 80:20 solutions were the same within the experimental error, as determined by the FTIR, XPS, ellipsometry, and NEXAFS experiments. SPR indicates that there were some small differences between these two surfaces that resulted in the carbohydrates being immobilized onto the PFPA-MUTEG/MDEG mixed film prepared from 90:10 solution in a concentration, orientation, or conformation that produced a higher biological activity.

IV. SUMMARY AND CONCLUSIONS

This article presents a detailed investigation of the chemical composition for the PFPA tailored surfaces. PFPA-MUTEG mixed with MDEG was assembled onto gold surfaces from solutions of different mole ratios. The resulting films were characterized by FTIR, XPS, ellipsometry, and NEXAFS. The results consistently show that the mixed PFPA-MUTEG/MDEG films prepared from the 90:10 and 80:20 solutions had the highest PFPA density, the mixed films were the thickest and the most homogeneous. While PFPA-MUTEG chains are relatively long and flexible, the addition of short MDEG chains appears to serve as a spacer facilitating the chain packing, thus increasing the packing density and order of the resulting film. SPR analysis of immobilized carbohydrates on the different PFPA modified surfaces shows the highest surface affinity for lectin on the PFPA-MUTEG/MDEG films prepared from 90:10 solutions. This demonstrates that the surface chemical composition of PFPA films can have a profound impact on the immobilization efficiency and function of the immobilized ligands.

ACKNOWLEDGMENTS

This research was funded by Oregon Nanoscience and Microtechnologies Institute (ONAMI) and ONR under Contract No. N00014-08-1-1237 and NIH (2R15GM066279, R01GM080295 and R01GM080295S1, P41EB002027). The authors also thank Tobias Weidner and Joe Baio for their expert technical assistance with the NEXAFS experiments. The NEXAFS experiments were performed at the NSLS, Brookhaven National Laboratory, which is supported by the U.S. Department of Energy, Division of Materials Science and Division of Chemical Sciences.

[1]J. P. Gann and M. Yan, Langmuir **24**, 5319 (2008).
[2]L.-H. Liu, G. Zorn, D. G. Castner, R. Solanki, M. M. Lerner, and M. Yan, J. Mater. Chem. **20**, 5041 (2010).
[3]J. Park and M. Yan, Acc. Chem. Res. **46**, 181 (2013).
[4]Y. Pei, H. Yu, Z. Pei, M. Theurer, C. Ammer, S. André, H.-J. Gabius, M. Yan, and O. Ramström, Anal. Chem. **79**, 6897 (2007).
[5]A. Tyagi, X. Wang, L. Deng, O. Ramström, and M. Yan, Biosens. Bioelectron. **26**, 344 (2010).
[6]H. Wang, Y. Zhang, X. Yuan, Y. Chen, and M. Yan, Bioconjugate. Chem. **22**, 26 (2011).
[7]X. Wang, O. Ramstörm, and M. Yan, Anal. Chem. **82**, 9082 (2010).
[8]L.-H. Liu and M. Yan, Acc. Chem. Res. **43**, 1434 (2010).
[9]S. A. Al-Bataineh, R. Luginbuehl, M. Textor, and M. Yan, Langmuir **25**, 7432 (2009).
[10]L. Liu, M. H. Engelhard, and M. Yan, J. Am. Chem. Soc. **128**, 14067 (2006).
[11]L.-H. Liu, M. M. Lerner, and M. Yan, Nano Lett. **10**, 3754 (2010).
[12]H. Wang, J. Ren, A. Hlaing, and M. Yan, J. Colloid Interface Sci. **354**, 160 (2011).
[13]J. C. Love, L. A. Estroff, J. K. Kriebel, R. G. Nuzzo, and G. M. Whitesides, Chem. Rev. **105**, 1103 (2005).
[14]A. Ulman, Chem. Rev. **96**, 1533 (1996).
[15]C. D. Bain and G. M. Whitesides, J. Am. Chem. Soc. **110**, 6560 (1988).
[16]P. E. Laibinis, M. A. Fox, J. P. Folkers, and G. M. Whitesides, Langmuir **7**, 3167 (1991).
[17]M.-W. Tsao, C. L. Hoffman, J. F. Rabolt, H. E. Johnson, D. G. Castner, C. Erdelen, and H. Ringsdorf, Langmuir **13**, 4317 (1997).
[18]M. Dhayal and D. M. Ratner, Langmuir **25**, 2181 (2009).
[19]C. D. Bain, H. A. Biebuyck, and G. M. Whitesides, Langmuir **5**, 723 (1989).
[20]J. F. Kang, S. Liao, R. Jordan, and A. Ulman, J. Am. Chem. Soc. **120**, 9662 (1998).
[21]J. Stöhr, *NEXAFS Spectroscopy* (Springer-Verlag, Berlin, 1992).
[22]G. Socrates, *Infrared and Raman Characteristic Group Frequencies, Tables and Charts*, 3rd ed. (Wiley, New York, 2001).
[23]D. Kessler, P. J. Roth, and P. Theato, Langmuir **25**, 10068 (2009).
[24]E. S. Gawalt, M. J. Avaltroni, N. Koch, and J. Schwartz, Langmuir **17**, 5736 (2001).
[25]R. G. Nuzzo, L. H. Dubois, and D. L. Allara, J. Am. Chem. Soc. **112**, 558 (1990).
[26]R. Adadi, G. Zorn, R. Brener, I. Gotman, E. Y. Gutmanas, and C. N. Sukenik, Thin Solid Films **518**, 1966 (2010).
[27]G. Zorn, I. Gotman, E. Y. Gutmanas, R. Adadi, G. Salitra, and C. N. Sukenik, Chem. Mater. **17**, 4218 (2005).
[28]See supplementary material at http://dx.doi.org/10.1116/1.4907924 for Table S1: XPS determined surface elemental compositions of 100% PFPA-MUTEG film, 100% MDEG film, and PFPA-MUTEG/MDEG mixed films prepared from solution concentrations of 90:10, 80:20, and 50:50; Fig. S1: Molecular structures of MUTEG; Table S2: XPS determined surface elemental compositions of the 100% PFPA-MUTEG film, 100% MUTEG film, and PFPA-MUTEG/ MUTEG mixed film prepared from a solution concentration of 90:10.
[29]G. Zorn, L.-H. Liu, L. Arnadottir, H. Wang, L. J. Gamble, D. G. Castner, and M. Yan, J. Phys. Chem. C **118**, 376 (2014).
[30]S. Uppalapati, S. Chada, M. H. Engelhard, and M. Yan, Macromol. Chem. Phys. **211**, 461 (2010).
[31]R. Winter, P. G. Nixon, G. L. Gard, D. J. Graham, D. G. Castner, N. R. Holcomb, and D. W. Grainger, Langmuir **20**, 5776 (2004).
[32]F. Cheng, L. J. Gamble, and D. G. Castner, Anal. Chem. **80**, 2564 (2008).
[33]P. M. Dietrich, N. Graf, T. Gross, A. Lippitz, B. Schüpbach, A. Bashir, C. Wöll, A. Terfort, and W. E. S. Unger, Langmuir **26**, 3949 (2010).
[34]J. A. Horsley, J. Stöhr, A. P. Hitchcock, D. C. Newbury, A. L. Johnson, and F. Sette, J. Chem. Phys. **83**, 6099 (1985).
[35]X. Li, L. Andruzzi, E. Chiellini, G. Galli, C. K. Ober, A. Hexemer, E. J. Kramer, and D. A. Fischer, Macromolecules **35**, 8078 (2002).
[36]A. C. Liu, J. Stöhr, C. M. Friend, and R. J. Madix, Surf. Sci. **235**, 107 (1990).
[37]D. A. Outka, J. Stöhr, R. J. Madix, H. H. Rotermund, B. Hermsmeier, and J. Solomon, Surf. Sci. **185**, 53 (1987).
[38]Y.-Y. Luk, N. L. Abbott, J. N. Crain, and F. J. Himpsel, J. Chem. Phys. **120**, 10792 (2004).
[39]D. Gupta, T. K. Dam, S. Oscarson, and C. F. J. Brewer, Biol. Chem. **272**, 6388 (1997).